








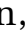
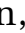
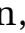












Long-Term Impacts of Invasive Insects and Pathogens on Composition, Biomass, and Diversity of Forests in Virginia's Blue Ridge Mountains

Kristina J. Anderson-Teixeira,^{1,2*}  Valentine Herrmann,¹  Wendy B. Cass,³  Alan B. Williams,³  Stephen J. Paull,³  Erika B. Gonzalez-Akre,¹  Ryan Helcoski,¹  Alan J. Tepley,^{1,4}  Norman A. Bourg,¹  Christopher T. Cosma,¹  Abigail E. Ferson,¹  Caroline Kittle,¹  Victoria Meakem,¹  Ian R. McGregor,¹  Maya N. Prestipino,¹  Michael K. Scott,¹  Alyssa R. Terrell,¹  Alfonso Alonso,⁵  Francisco Dallmeier,⁵  and William J. McShea¹ 

¹Conservation Ecology Center, Smithsonian Conservation Biology Institute and National Zoological Park, 1500 Remount Rd. MRC 5535, Front Royal, Virginia 22630, USA; ²Center for Tropical Forest Science-Forest Global Earth Observatory, Smithsonian Tropical Research Institute, Panama, Republic of Panama; ³Shenandoah National Park, 3655 US Hwy 211 East, Luray, Virginia 22835, USA; ⁴Natural Resources Canada, Canadian Forest Service, Northern Forestry Centre, 5320 122 St., Edmonton, Alberta T6H 3E5, Canada; ⁵Center for Conservation and Sustainability, Smithsonian Conservation Biology Institute, National Zoological Park, Washington, District of Columbia, USA

ABSTRACT

Exotic forest insects and pathogens (EFIP) have become regular features of temperate forest ecosystems, yet we lack a long-term perspective on their net impacts on tree mortality, carbon sequestration, and tree species diversity. Here, we

analyze 3 decades (1987–2019) of forest monitoring data from the Blue Ridge Mountains ecoregion in eastern North America, including 67 plots totaling 29.4 ha, along with a historical survey from 1939. Over the past century, EFIP substantially affected at least eight tree genera. Tree host taxa had anomalously high mortality rates ($\geq 6\%$ year⁻¹ from 2008 to 2019 vs 1.4% year⁻¹ for less-impacted taxa). Following the arrival of EFIP, affected taxa declined in abundance (– 25 to – 100%) and live aboveground biomass (AGB; – 13 to – 100%) within our monitoring plots. We estimate that EFIP were responsible for 21–29% of ecosystem AGB loss through mortality (– 87 g m⁻² year⁻¹) from 1991 to 2013 across 66 sites. Over a century, net AGB loss among affected species totaled roughly 6.6–10 kg m⁻². The affected host taxa ac-

Received 25 January 2020; accepted 22 March 2020

Electronic supplementary material: The online version of this article (<https://doi.org/10.1007/s10021-020-00503-w>) contains supplementary material, which is available to authorized users.

Authors' contributions: KJAT, WBC, AJT, and VH conceived and designed the study; WBC, EBGA, NAB, AA, FD, and WJM designed and implemented forest monitoring protocols; AW, SJP, RH, EBGA, NAB, CTC, AEF, CK, VM, IRM, MNP, MKS, and ART performed the research; VH and KJAT analyzed the data; KJAT led the writing of the manuscript. All authors reviewed and approved the draft.

*Corresponding author; e-mail: teixeirak@si.edu

counted for 23–29% of genera losses at the plot scale, with mixed net effects on α -diversity. Several taxa were lost from our monitoring plots but not completely extirpated from the region. Despite these losses, both total AGB and α -diversity were largely recovered through increases in sympatric genera. These results indicate that EFIP have been an important force shaping forest composition, carbon cycling, and diversity. At the same time, less-affected taxa in these relatively diverse temperate forests have conferred substantial resilience with regard to biomass and α -diversity.

Key words: temperate forest; invasives; forest insect pests; forest pathogens; tree mortality; diversity; biomass; carbon; conservation.

HIGHLIGHTS

- Exotic forest pests have substantially impacted at least 24% of tree genera ($n = 8$).
- Exotic forest pests were linked to 21–29% of biomass losses in recent decades.
- Exotic forest pests had mixed effects on tree biodiversity.

INTRODUCTION

Forests harbor the majority of terrestrial biodiversity and play a critical role in climate regulation (Hassan and others 2005; Bonan 2008), yet their future is uncertain in the face of multiple anthropogenic global change pressures (for example, Sala 2000; Friedlingstein and others 2006). One of the largest and most imminent hazards to temperate forest health is exposure to exotic forest insects and pathogens (EFIP), which can cause extensive tree mortality and substantially impact forest structure, tree diversity, and energy, water, carbon, and nutrient fluxes (Boyd and others 2013; Lovett and others 2016; Seidl and others 2018; Fei and others 2019). They can also have massive economic and societal costs (Bradshaw and others 2016).

Exotic insects and pathogens have become common features of most temperate forest ecosystems worldwide (Boyd and others 2013). In the USA, at least 471 EFIP have been documented since 1635 (Aukema and others 2010), with up to 45 invasive EFIP in some counties of the northeast (Liebhold and others 2013). Each invasion has impacted host taxa that evolved in isolation from the insect or pathogen

and lack defense mechanisms, at times virtually eliminating once-abundant tree genera from the landscape (Lovett and others 2006). For example, American chestnut (*Castanea dentata*) has been eliminated as a canopy species in the eastern USA by chestnut blight (Anagnostakis 1987), eastern hemlock (*Tsuga canadensis*) is experiencing severe declines across much of its native range (Ellison and others 2018) due to the hemlock woolly adelgid, and ash trees (*Fraxinus* spp.) are currently being decimated by emerald ash borer (Herms and McCullough 2014). EFIP invasions are expected to continue for the foreseeable future, driven by ever-increasing global trade and travel along with associated EFIP introductions (Levine and D'Antonio 2003; Aukema and others 2010; Boyd and others 2013) and probable exacerbation by climate change (Ayres and Lombardero 2000; Dukes and others 2009; Seidl and others 2018).

Despite their prevalence and potentially damaging effects, relatively little is known regarding the net impacts of EFIP on forest composition, biomass, and diversity (Peltzer and others 2010), particularly over the long term (Strayer and others 2006). The effects of individual EFIP disturbances have previously been quantified, most commonly with emphasis on stands where the impact is particularly severe (for example, Flower and others 2013; Finzi and others 2014), and there are regional assessments of recent (post-2004) impacts and threats of multiple EFIP (Fei and others 2019; Potter and others 2019). However, we are unaware of any study that has characterized the aggregate long-term impacts of multiple EFIP on forest composition, biomass, and diversity.

Here, we draw on long-term forest monitoring plots throughout Shenandoah National Park (SNP) and at the adjacent Smithsonian Conservation Biology Institute (SCBI) to characterize the impacts of multiple EFIP on forests within the Appalachian/Blue Ridge Mountains ecoregion. Combined, our records include more than 350,000 tree observations over 3 decades (1987–2019), with a total sample area of 29.4 ha distributed throughout the 81,900 ha study region. We focus on eight tree genera that were substantially impacted by EFIP over the past century (Table 1). For outbreaks that peaked prior to the start of our quantitative records, we supplement our quantitative data with qualitative species abundance descriptions from an SNP vegetation survey in 1939 (Berg and Moore 1941). We address three major questions regarding the impact of exotic insects and pathogens: (1) How has each tree host taxa been impacted in terms of abundance, live aboveground biomass (henceforth,

Table 1. Impactful Exotic Forest Insects and Pathogens in the Blue Ridge Mountains

| Insect/ pathogen(s) | Host species | Insect/pathogen type | Origin | Years of outbreak in study region | References |
|---|---|------------------------|---|--|---|
| Chestnut blight (<i>Cryphonectria parasitica</i> (Murrill) Barr) | American chestnut (<i>Castanea dentata</i> (Marshall) Borkh) | Fungal/stem rot | Asia | Mid-1920s (still pre-sent) | Anagnostakis (1987) |
| Dutch elm disease (<i>Ophiostoma</i> spp. ^a) | Elm (<i>Ulmus americana</i> L., <i>Ulmus rubra</i> Muhl.) ^b | Fungal/stem rot | Asia | Likely 1940s to present | Brasier (1991, 2000) |
| <i>Neofusicoccum</i> spp. (previously <i>Botryosphaeria</i> spp.) | Redbud (<i>Cercis canadensis</i> L.) | Fungal/stem rot | Unknown (globally distributed) ^c | Unknown (by 1950 in D.C.; currently present) | Wester and others (1950); Sakalidis and others (2013) |
| Butternut canker (<i>Ophiognomonia clavignenti-juglandacearum</i> (N.B. Nair, Kostichka & J.E. Kuntze Broders & Bolland) | Butternut (<i>Juglans cinerea</i> L.) | Fungal/stem rot | Asia | Likely 1970s to present | Morin and others (2018) |
| Dogwood anthracnose pathogen (<i>Discula destructiva</i> Redlin) | Dogwood (<i>Cornus florida</i> L., <i>Cornus alternifolia</i> L. f.) | Fungal/stem rot | Asia | Likely mid-1980's to present | Caetano-Anollés and others (2001), Carr and Bannas (2000) |
| Gypsy moth (<i>Lymantria dispar</i> L.) | Oaks (<i>Quercus</i> spp.; 11 species) | Insect/defoliator | Europe | 1984–1995 (still present) ^d | Kasbohm (1994) |
| Hemlock woolly adelgid (<i>Adelges tsugae</i> (Annand)) | Hemlock (<i>Tsuga canadensis</i> (L.) Carrière) | Insect/phloem feeder | Asia | 1988–2007 (still present) | Ellison and others (2018) |
| Emerald ash borer (<i>Agrilus planipennis</i> Fairmaire) | Ash (<i>Fraxinus americana</i> L., <i>F. nigra</i> Marshall, <i>F. pennsylvanica</i> Marshall) | Insect/xylem disruptor | Asia | 2013–present | Herms and McCullough (2014) |

Criteria for inclusion are detailed in Appendix S1.

^aCausal agents include *Ophiostoma ulmi* (Buisman) Nannf, *Ophiostoma novo-ulmi* Brasier, and *Ophiostoma himal-ulmi* Brasier & M.D. Mehrotra. Vectors include *Scolytus multistriatus* (Marshall) (exotic), *Scolytus schevyrewi* Semenov (exotic), and *Hylurgopinus rufipes* (Eichhoff) (native).

^b*Ulmus americana* is more vulnerable than *Ulmus rubra*, but both are affected. The taxa are also affected by elm yellows (*Ophiostoma ulmi* (Buisman) Melin & Nannf. And *O. novo-ulmi* Brasier), but we do not have any definitive evidence of this disease within our monitoring plots.

^cThe *Neofusicoccum* species complex affects orchard species and is globally distributed, with frequent movement across international borders (Sakalidis and others 2013). The most widespread is *N. parvum* Pennycook and Samuels.

^dThe first and largest outbreak occurred from 1984 to 95 and was suppressed in 1995 through the spraying of *Bacillus thuringiensis* var. *curstaki*. Thereafter, populations have largely been kept in check by the naturally occurring fungal pathogen: *Entomophaga maimaga* Humber, Shimazu, and Soper. There have been smaller subsequent outbreaks.

AGB), and mortality rate?; (2) How have EFIP affected ecosystem-level AGB?; and (3) How have EFIP altered tree biodiversity at the stand level (α -diversity) and landscape scale (γ -diversity)?

MATERIALS AND METHODS

Study Sites and Data

Our study sites included long-term forest monitoring plots throughout Shenandoah National Park

(SNP) and at the adjacent Smithsonian Conservation Biology Institute (SCBI), which together are distributed across an approximately 130 km stretch of the Appalachian/Blue Ridge Mountains ecoregion spanning 38.12–38.89°N latitude and 78.14–78.77°W longitude (Figure 1). Terrain is mountainous, with elevations of our study plots ranging from 273 to 1097 m.a.s.l. Climate is humid warm temperate (Köppen zone Cfa) with temperate oceanic (Cfb) and warm-summer humid conti-

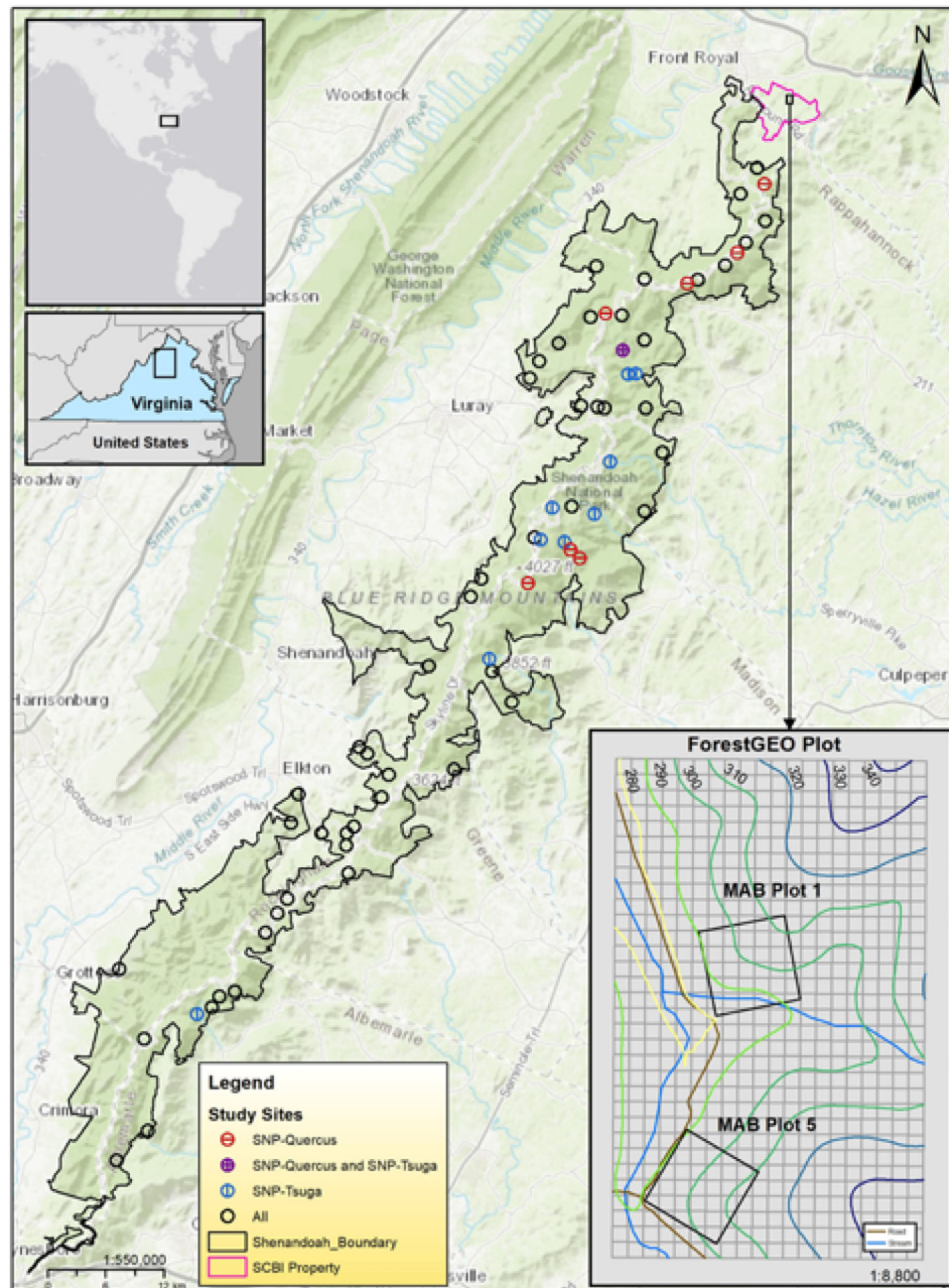


Figure 1. Map of the study region and plots within Shenandoah National Park (SNP) and the Smithsonian Conservation Biology Institute (SCBI). Plot details are given in Table 2.

mental (Dfa) climates at higher elevations. The region is mostly forested, including broadleaf deciduous, mixed, and conifer forests. Dominant tree genera currently include oaks (*Quercus montana* Willd, *Quercus rubra* L.), tulip poplar (*Liriodendron tulipifera* L.), maples (*Acer rubrum* L., *Acer saccharum* Marshall), birch (*Betula alleghaniensis* Britton, *Betula lenta* L.), black gum (*Nyssa sylvatica* Marshall), ash (*Fraxinus americana*, *F. pennsylvanica*), black locust (*Robinia pseudoacacia* L.), basswood (*Tilia americana*

L.), and hickories (*Carya glabra* (Mill.) Sweet, *Carya cordiformis* (Wangenh.) K. Koch, *Carya tomentosa* (Lam.) Nutt., *Carya ovalis* (Wangenh.) Sarg., *Carya ovata* (Mill.) K. Koch) (Cass and others 2012; Young and others 2009). Forests are mostly mature secondary, having undergone logging, agricultural clearing, and use for small-scale farms and pasture prior to establishment of SNP in 1935 and SCBI in 1975 (Connors 1988; Bourg and others 2013).

The vegetation of SNP was surveyed shortly after the Park's establishment, with qualitative abundance descriptors reported by species (Berg and Moore 1941). Quantitative censuses of trees at least 10 cm in permanent plots began in 1987, as detailed in Appendix S2. We focus here on 66 24×24 m plots that have been continuously censused since at least 1991 (SNP-66; Figure 1; Table 2), which constitute 41% of current monitoring sites selected to represent a stratified sample of bedrock geology type, slope aspect, and elevation in the current monitoring scheme (Mahan and others 2007). We also examine subsets of these 66 plots to characterize the impacts of the gypsy moth (SNP-*Quercus*; $n = 8$) and the hemlock woolly adelgid (SNP-*Tsuga*; $n = 10$; Table 2). At SCBI, we evaluate two 1-ha forest monitoring plots established in 1995 (SCBI-MAB), as well as the 25.6-ha ForestGEO vegetation dynamics plot into which they were incorporated in 2008 (SCBI-ForestGEO; Figure 1), all of which were subdivided into 20×20 m quadrats. While limited to a single site ($38^\circ 53' 36.6''$ N, $78^\circ 08' 43.4''$ W), the SCBI records capture smaller individuals (≤ 1 cm), cover a large contiguous area, and include detailed annual monitoring of tree mortality and its causes since 2014 (Table 2).

Analyses

Aboveground biomass of individual trees was calculated using allometric equations selected from existing compilations for North America (Jenkins and others 2003; Chojnacky and others 2014), giving precedence to taxa-specific and local allometric equations as described by Gonzalez-Akre and others (2016). Abundance and AGB (Mg dry biomass) per genus and for all species combined were summed across each 24×24 m SNP plot or 20×20 m quadrat at SCBI (640 total in ForestGEO plot) and linearly interpolated across censuses to create time series. Annual stem mortality rate (m ; % year⁻¹), biomass mortality (g m⁻² year⁻¹), and woody aboveground net primary productivity, ANPP_{woody} (g m⁻² year⁻¹), were calculated as in Gonzalez-Akre and others (2016) when individual trees were reliably tracked (Table 2). We limited our calculation of m to cases when at least 100 individuals at least 10 cm DBH were present per genus at SCBI-ForestGEO.

The annual net change in AGB, Δ AGB, is the balance between AGB losses (that is, woody mortality) and gains from growth and recruitment (ANPP_{woody}). However, because tree mortality is rare and our plots/quadrats are relatively small and

diverse, we expected that mortality would dominate Δ AGB within any given genera, plot, and census interval in which it occurs, such that genera-specific Δ AGB values would approach woody mortality when negative (Δ AGB⁻) and ANPP_{woody} when positive (Δ AGB⁺). This logic was verified by comparing Δ AGB⁻ and Δ AGB⁺ with woody mortality and ANPP_{woody}, respectively, when the latter could be calculated.

We quantified α - and γ -diversity at the genus level using the presence-absence metrics. Specifically, for each set of plots, α -diversity was defined as the number of genera present within each plot (SNP) or 20×20 -m sampling quadrat (SCBI), and γ -diversity was defined as the total number of genera present within each set of plots (Table 2).

For tree taxa subjected to an EFIP outbreak more than a decade prior to the start of our records (before the mid-1980s), we used the 1939 vegetation survey of Berg and Moore (1941) to roughly estimate historical abundance and biomass, as detailed in Appendix S3.

Attribution of Losses to EFIP

We identified EFIP-tree host combinations (Table 1) that met three criteria, as detailed in Appendix S1: (1) The insect or pathogen was exotic in origin and transported to the region by human activities; (2) the presence of the EFIP was confirmed within our specific study area through observations of the insect/pathogen or its signatures on dead or declining host trees; (3) the host taxa had suffered substantial ($> 20\%$) decline in abundance or displayed elevated mortality rates ($> 5\%$ year⁻¹) concurrent with EFIP presence. Because most of the EFIP considered here affected all species within a genus that were present in our plots, and because not all trees were successfully identified to species during the forest censuses, we conducted analyses at the genus level. An exception was the genus *Juglans*, including *J. cinerea* (heavily impacted by butternut canker) and *J. nigra* L. (little impacted); these species were treated separately.

Losses occurring within a host tree genus during the time period over which the associated EFIP was present (Tables 1, S1) were classified as *EFIP-associated*, and the rest as *EFIP-unlikely*. For Δ AGB⁻ and α -diversity losses, the *EFIP-associated* category was subdivided into *EFIP-likely*, referring to losses exceeding typical rates of "background" mortality and likely due to EFIP, and *EFIP-possible*, referring to losses likely to have occurred regardless of the presence of EFIP, even if EFIP induced. Losses were

Table 2. Forest Census Plots Analyzed Here

| Code | Description | Role in analyses | Plot size | N plots | Dates analyzed ^a | Census frequency | Minimum DBH _{min} (cm) | Individual tracking ^b | References |
|---------------------|--|--|-----------|---------|-----------------------------|------------------------------------|---------------------------------|----------------------------------|--|
| SNP-66 | Subset of long-term ecological monitoring system plots | Focal SNP plots | 24 × 24 m | 66 | 1991–2013 | ~ Every 4 years | 10 | Starting 2003 | Cass and others (2011) |
| SNP- <i>Quercus</i> | Subset of SNP-66 plots dominated by <i>Quercus</i> | Characterize gypsy moth impacts | 24 × 24 m | 8 | 1987–2013 | ~ Every 4 years | 10 | Starting 2003 | Cass and others (2011) |
| SNP- <i>Tsuga</i> | Subset of SNP-66 plots containing <i>Tsuga</i> | focus on hemlock woolly adelgid impacts | 24 × 24 m | 10 | 1991–2013 | ~ Every 4 years | 10 | Starting 2003 | Cass and others (2011) |
| SCBI-MAB | Plots established as part of the Smithsonian's Monitoring and Assessment of Biodiversity Program | long-term record at SCBI | 1 ha | 2 | 1995–2018 | 1995, then same as SCBI-For-estGEO | 4 | Starting 2008 | - |
| SCBI-For-estGEO | Forest Global Earth Observatory (ForestGEO) large forest dynamics plot | Capture smaller individuals and large area | 25.6 ha | 1 | 2008–2018 | Every 5 years | 1 | Yes | Bourg and others (2013); Anderson-Teixeira and others (2015) |
| | | Characterize recent mortality rates and causes | 25.6 ha | 1 | 2014–2019 | Annual | 10 ^c | Yes | Gonzalez-Akre and others (2016) |

Plots are mapped in Figure 1, and details are provided in Appendix S2.

^aFor SNP, census intervals were staggered, and numbers refer to range of dates with available estimates for all plots.

^bTracking of individuals allows calculation of mortality rate, woody mortality, and ANPP_{woody}.

^cCensused down to DBH = 1 cm for *Fraxinus*.

partitioned through multiplication by a weighting factor representing the fraction of losses above “background” mortality, f_{efip} (Table S4). Specifically, f_{efip} was calculated as $f_{\text{efip}} = 1 - m_b/m_{\text{efip}}$, where m_b is likely “background” mortality and m_{efip} is total observed mortality during a time when the EFIP was present. For genera for which our records covered periods both with and without EFIP (*Quercus*, *Fraxinus*), m_b was defined based on the period without EFIP. For all other taxa, m_b was defined as the average mortality rate observed at SCBI across all species unaffected by EFIP (1.4% year⁻¹). For genera present in the SCBI-ForestGEO plot and affected by EFIP between 2008 and 2019 (*Ulmus*, *Cercis*, *Cornus*, and *Fraxinus*), m_{efip} was calculated from our mortality census data. For *Tsuga*, 100% mortality by 2007 was compared to mortality that would have been expected over the same period at the background rate. For *Quercus*, for which we lacked mortality rate data during the EFIP outbreak, m_{efip} and m_b were defined as ΔAGB^- during EFIP and non-EFIP periods, respectively. For *Castanea*, m_{efip} could not be calculated, so, given the lethality of chestnut blight, we assigned f_{efip} equal to the maximum among the other species. For ΔAGB , the null expectation is that “background” mortality (or ΔAGB^-) is balanced by growth (ΔAGB^+), resulting in zero net change, so EFIP-associated losses were not partitioned.

RESULTS

Identification of Focal EFIP–Tree Host Pairs

We identified eight EFIP with host taxa that had undergone substantial decline over the past century (Tables 1, 3). With the exception of chestnut blight, characteristic symptoms of all EFIP agents were observed on dead or declining trees within our study plots (Tables 2, S1; Figure 2). There were six additional EFIP–host tree combinations where the insect/pathogen was confirmed present in our study region but for which we lacked evidence of significant EFIP-attributable decline in the host species (Table S2). Two tree genera, *Pinus* and *Robinia*, suffered more than 20% declines in the SNP-66 plots, but these declines were primarily attributable to causes other than EFIP (Appendix S2). All tree genera experiencing more than 5% year⁻¹ mortality rates during any census period at the SCBI-ForestGEO plot had documented EFIP, with the exception of *Carpinus caroliniana* in 2019 (cause uncertain) (Figure 2).

Impacts on Tree Taxa

Three previously important canopy taxa: *C. dentata*, *Ulmus* spp., and *J. cinerea*, were affected by exotic pathogens that established in the region prior to the start of our records (Table 3). In 1939, *C. dentata* was described as “previously abundant,” with AGB estimated at roughly 1.6–5 kg m⁻², prior to the arrival of the chestnut blight (Tables 3, S3). *C. dentata* individuals at least 10 cm DBH disappeared from the SNP-66 plots in 2010, but repeated formation of short-lived sprouts from long-dead stumps maintained smaller individuals throughout the region. Where smaller trees were sampled at SCBI-ForestGEO, several of such sprouts persisted at DBH at least 1 cm through 2018 (Appendix S4).

Ulmus americana and *U. rubra* were both described as “sparse” in 1939, prior to arrival of Dutch elm disease, corresponding to an estimated AGB of roughly 0.3 kg m⁻² (Tables 3, S3). Within the time frame of our records, they persisted at low densities (Table 3), low biomass, and increasingly small sizes (Appendix S4). *U. americana* constituted 8% and 4% of living *Ulmus* spp. in the most recent censuses at SNP-66 and SCBI-ForestGEO, respectively. At SCBI, the genera had an anomalously high mortality rate of 14.1% year⁻¹ for stems at least 10 cm from 2008 to 2019, compared to a mean of 1.4% year⁻¹ across all species with no documented EFIPs (Figure 2A). Recently dead individuals displayed symptoms of Dutch elm disease (Figure 2B).

Juglans cinerea was described as “common” in 1939 prior to the arrival of butternut canker, corresponding to AGB of roughly 0.8 kg m⁻² (Tables 3, S3). It was never recorded in the SNP-66 plots, and in the SCBI-ForestGEO plot, it declined from four living individuals in 2008 to two in 2018 (max DBH = 28 cm in both years).

Two small tree genera: *Cornus* and *Cercis*, were affected by fungal pathogens and exhibited declining trends and high mortality throughout the course of the study period. *Cornus* declined dramatically in most individual plots and on average in all sets of plots—up to 90% from 1995 to 2018 in the SCBI-MAB plots (Figure 3E, F, Appendix S4). *Cercis* exhibited more modest but still substantial declines (Appendix S4)—up to 76% from 1995 to 2018 for stems at least 4 cm in the SCBI-MAB plots. At SCBI, recent (2008–2019) mortality rates of stems at least 10 cm averaged 7.1% year⁻¹ for *Cornus* and 6.2% year⁻¹ for *Cercis*, with recently dead individuals displaying signs of fungal pathogens (Figure 2).

Table 3. Changes in Average Abundance and Biomass of EFIP Host Taxa in Shenandoah National Park

| Host taxa | Insect/ pathogen evidence ^a | Censuses | | Abundance ($n \geq 10$ cm DBH per 100 m ⁻²) | | | Live aboveground biomass (AGB) (kg m ⁻² —stems ≥ 10 cm) | | |
|---------------------------------------|--|-----------------------|---------------------|--|-----------------|--------------------|--|-----------------|-----------------------------|
| | | Pre-invasion | Post-invasion | Pre-invasion | Post-invasion | Net loss | Pre-invasion | Post-invasion | Net loss (Δ AGB) |
| <i>Castanea dentata</i> | P | Berg and Moore (1941) | 2013 | “Previously abundant” | 0 | – | ~ 1.6 – ^{5b} | 0 | ~ 1.6 – ^{5b} |
| <i>Ulmus</i> spp. | S,P | Berg and Moore (1941) | 2013 | “Sparse” (both <i>U. americana</i> and <i>rubra</i>) | 0.04 ± 0.01 | – | $\sim 0.32^b$ | 0.04 ± 0.1 | $\sim 0.28^b$ |
| <i>Cercis canadensis</i> ^c | S,P | – | 2013 | – | 0 | 0.008 ^c | – | 0 | 0.006 ^c |
| <i>Juglans cinerea</i> | S,P | Berg and Moore (1941) | 2013 | “Common” | 0 | – | $\sim 0.8^b$ | 0 | $\sim 0.8^b$ |
| <i>Cornus</i> spp. | S,P | 1991 | 2013 | 0.11 ± 0.03 | 0.02 ± 0.01 | 0.09 | 0.05 ± 0.14 | 0.01 ± 0.05 | 0.04 |
| <i>Quercus</i> spp. | O,S,P | 1987 | 1995 | 1.9 ± 2.0^d | 1.4 ± 1.6 | 0.5 | 11.4 ± 11.6^d | 9.9 ± 10.1 | 1.5^d |
| <i>Tsuga canadensis</i> | O,S,P | 1991 | 2013 | 0.3 ± 1.0 | 0 | 0.3 | 0.9 ± 0.3 | 0 | 0.9 |
| <i>Fraxinus</i> spp. | O,S,P | 2013 | (2025) ^e | 0.23 ± 0.05 | 0 ^e | 0.23 ^e | 1.5 ± 3.4 | 0 ^e | 1.5^e |

Census data refer to individuals ≥ 10 cm DBH in the SNP-66 plots.^aO—direct observation of insect/pathogen at our research sites, S—observation of typical signs of insect/pathogen on dead/declining trees of the host genus at our research sites, P—the presence in the region. Details are given in Table S1.^bPre-invasive AGB was estimated from Berg and Moore (1941) as described in Appendix S3.^cPre-invasion abundance and AGB were not estimated because it is unknown whether the pathogen was present at the time of the Berg and Moore (1941) survey and because their description of its abundance is inadequate for linking to a current equivalent. Estimates of change given here refer to losses in the SNP-66 within the time frame of our quantitative records.^dEstimates assume that the proportional loss of oak abundance (17.7%) and AGB (11.2%) observed in SNP-Quercus plots from 1987 to 91 was representative across the SNP-66 plots. Given heterogeneity across the landscape, this estimate has high uncertainty.^eEstimates assume that there will be near-complete loss of *Fraxinus* ≥ 10 cm DBH (Abella and others 2019).

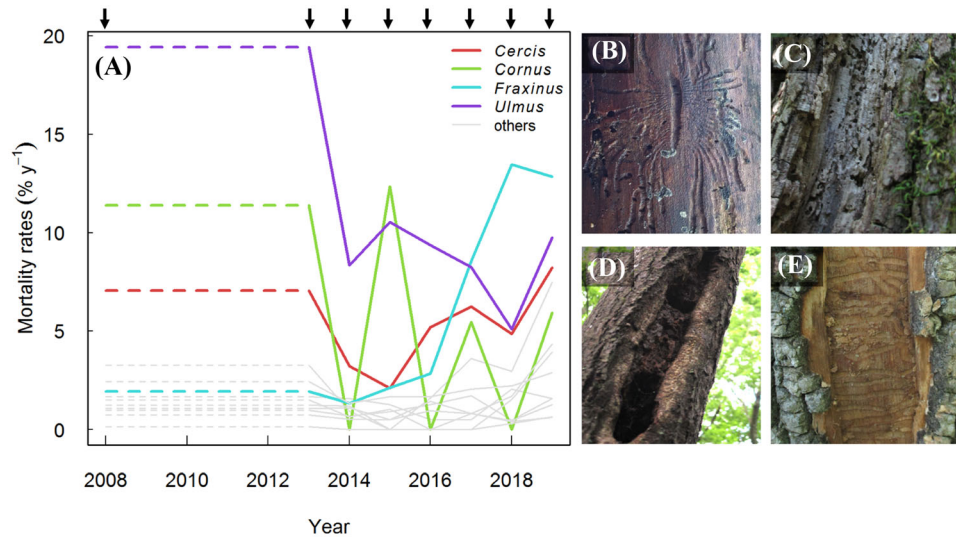


Figure 2. Elevated tree mortality rates attributable to exotic insects and pathogens in the SCBI-ForestGEO plot from 2008 to 2019. **A** Mortality rates of trees ≥ 10 cm DBH, with genera affected by EFIP during this time period (Table 1) shown in color and others in grey. Included are genera with $N \geq 100$ individuals in 2008, with the exception of focal taxa *Cornus* ($N_{2008} = 29$). Dashed line indicates annualized mortality rate for the period prior to initialization of the annual census. Arrows on upper axis indicate census years. Impact of the insect/pathogen was confirmed through observations of signs and symptoms of the disease on recently dead individuals: **B** gallery of Dutch elm disease vector *Scolytus multistriatus* on *Ulmus rubra*; fungal cankers/stem rot on **C** *Cornus florida* and **D** *Cercis canadensis*, and **E** *Agrilus planipennis* galleries under the bark of *Fraxinus americana*.

Quercus declined between 1987 and 1995, concurrent with a gypsy moth infestation (Figure 3A, B). In the SNP-*Quercus* plots (Table 2), losses during this period averaged 24.9% of individuals and 15% of AGB. Assuming that percent loss rates for *Quercus* in SNP-*Quercus* plots were representative across the SNP-66 plots, we estimate $\Delta \overline{\text{AGB}} \approx -1.5 \text{ kg m}^{-2}$ during this outbreak across SNP-66 plots. After 1995, *Quercus* AGB increased gradually over most of the study period (Figure 3B). These increases were driven by individual tree growth as opposed to new recruitment. *Quercus* tree density continued to decline slowly after 1995 (Figure 3A), but these declines were not attributed to gypsy moths.

Tsuga was initially present in ten of SNP-66 plots (Figure 3C, D), in which its 1991 AGB averaged 5.9 kg m^{-2} and ranged from 0.1 to 15.9 kg m^{-2} (0.4–55% total AGB). It underwent sharp decline from 1994 to 2007, beyond which live individuals were no longer recorded in SNP-66 monitoring plots, although more than 20,000 insecticide-treated trees remain alive throughout SNP.

Fraxinus mortality attributed to the emerald ash borer was captured in SCBI censuses (Figure 3G, H). In 2013, prior to the start of its decline, *Fraxinus* AGB was increasing at SNP and stable at SCBI (Figures 4, S1). Stems at least 10 cm DBH averaged

0.23 individuals per 100 m^2 and $1.4 \text{ kg AGB m}^{-2}$ across the SNP-66 plots (Table 3) and 0.34 individuals per 100 m^2 and $1.7 \text{ kg AGB m}^{-2}$ at SCBI-ForestGEO (Figure 4). At SCBI, emerald ash borer-driven mortality was first detected in 2016 and accelerated steeply thereafter, exceeding $12.5\% \text{ year}^{-1}$ for stems at least 10 cm in 2018 and 2019 (Figure 2). As of 2019, *Fraxinus* had lost 28% of individuals and 30% of AGB (relative to 2016), and 95% of remaining live trees were categorized as “unhealthy.”

Impacts on Carbon Cycling

EFIP were associated with substantive portions of recorded AGB losses (Figure 4). The variable ΔAGB^- , which we use to approximate AGB losses due to tree mortality, captured the majority of biomass mortality during periods for which the latter could be calculated (Table 2; Figure 4). In SNP, EFIP were associated with 29% (21% EFIP-likely, 8% EFIP-possible) of ΔAGB^- from 1991 to 2013 in the SNP-66 plots (Figure 4A–C), corresponding to an average loss rate of $-87 \text{ g m}^{-2} \text{ year}^{-1}$. In SNP-*Quercus* and SNP-*Tsuga* plots, EFIP were associated with much higher fractions of ΔAGB^- : 49% (41% EFIP-likely; Figure 4D–F) and 55% (41% EFIP-likely; Figure 4I), respectively. At SCBI, EFIP were associated with only 8% (6%

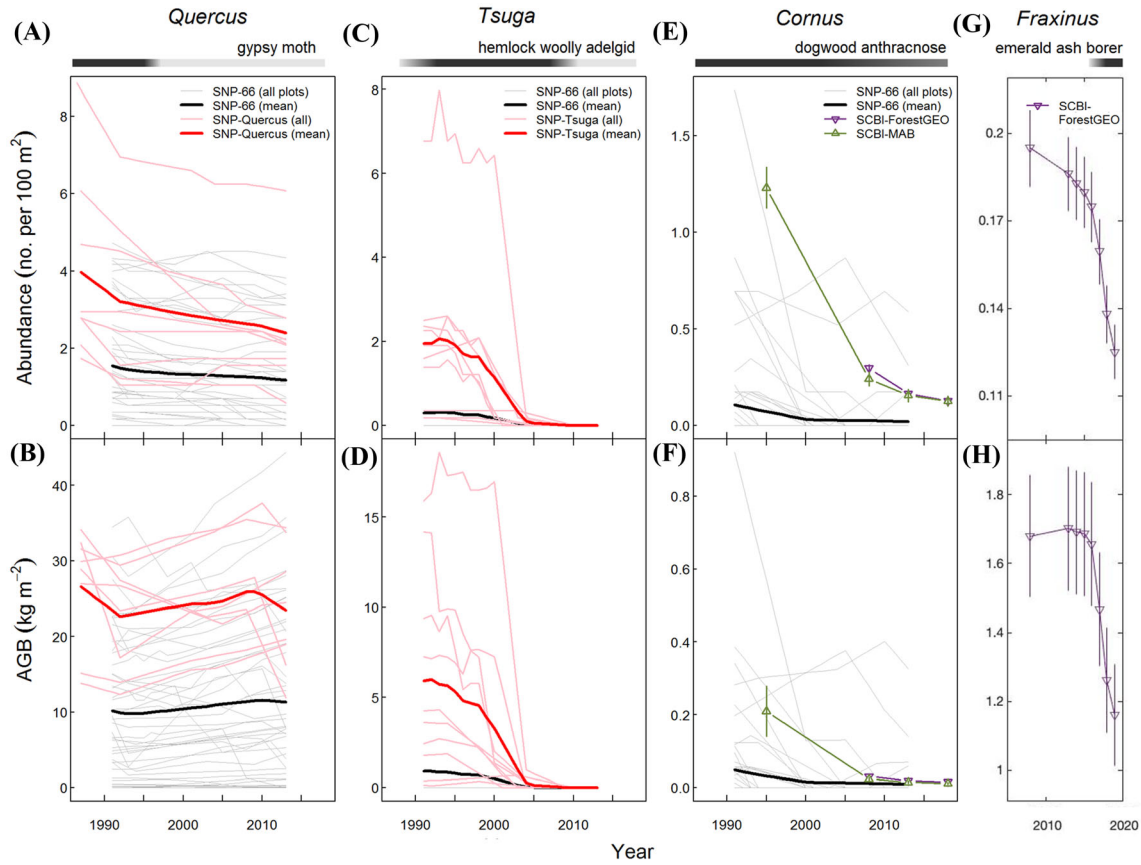


Figure 3. Trends in abundance and biomass for four genera impacted by EFIP since 1989: **A, B** *Quercus*, **C, D** *Tsuga*, **E, F** *Cornus*, and **G, H** *Fraxinus*. Trends for all individual SNP-66 plots are shown (thin lines; not plotted for *Fraxinus* because SNP-66 record does not capture emerald ash borer outbreak), along with means across all sites and across *SNP-Quercus* or *SNP-Tsuga* plots. For *Cornus* and *Fraxinus*, trends at SCBI are also plotted, where error bars indicate ± 1 SE of the mean across subplots. Minimum DBH is as in Table 2. Note that y-axes differ. Shaded bars at the top of the figure indicate the relative intensity through time of the EFIPs.

EFIP-likely; Figure 4J–L) of ΔAGB^- in the MAB plots (1995–2018) and 24% (19% *EFIP-likely*; Figure 4M–O) of ΔAGB^- across the full ForestGEO plot (2008–2018).

Shifting focus from ΔAGB^- to net changes in average AGB ($\overline{\Delta\text{AGB}}$) across the SNP-66 plots, EFIP were associated with $\overline{\text{AGB}}$ loss of roughly 6.6–10 kg m^{-2} , or on average about 66–100 $\text{g m}^{-2} \text{ year}^{-1}$, over the about 100-year period from the arrival of chestnut blight in the mid-1920s through the anticipated near-total loss of *Fraxinus* (by ~ 2025 ; Table 3). Of this, roughly 2.7–6.0 kg AGB m^{-2} was lost starting prior to the start of our quantitative records in 1987, including about 1.6–5.0 kg m^{-2} from *C. dentata*, about 0.8 kg m^{-2} from *J. cinerea*, and about 0.3 kg m^{-2} from *Ulmus* spp. (Table 3). These estimates have very high uncertainty (Appendix S3, Tables 3, S3). Losses recorded in our quantitative records total 2.4 kg m^{-2} : $\sim 1.5 \text{ kg m}^{-2}$ from *Quercus*, 0.9 kg m^{-2} from

Tsuga, 0.04 kg m^{-2} from *Cornus*, and less than 0.01 kg m^{-2} from *Cercis*. *Fraxinus* AGB averaged 1.5 kg m^{-2} across the SNP-66 plots in 2013, predicted to be mostly or completely lost within the next decade.

Despite EFIP-associated losses, average AGB increased by 2.6 kg m^{-2} between 1991 and 2013 across the SNP-66 plots (Figure 4B, C). Taxa with the largest $\overline{\Delta\text{AGB}}$ during this period included *Liriodendron* (1.7 kg m^{-2}), *Quercus* (1.2 kg m^{-2}), *Fraxinus* (0.6 kg m^{-2}), *Betula* (0.4 kg m^{-2}), and *Acer* (0.3 kg m^{-2}). The more heavily impacted *SNP-Quercus* and *SNP-Tsuga* plot sets experienced net $\overline{\text{AGB}}$ losses (-1.4 and -4.8 kg m^{-2} , respectively; Figure 4F, I). In contrast, at SCBI, where EFIP impacts on AGB were relatively minor, $\overline{\text{AGB}}$ increased by 7.4 kg m^{-2} between 1995 and 2018 in the MAB plots (Figure 4K, L) and by 2.6 kg m^{-2} between 2008 and 2018 across the full ForestGEO plot (Figure 4N, O).

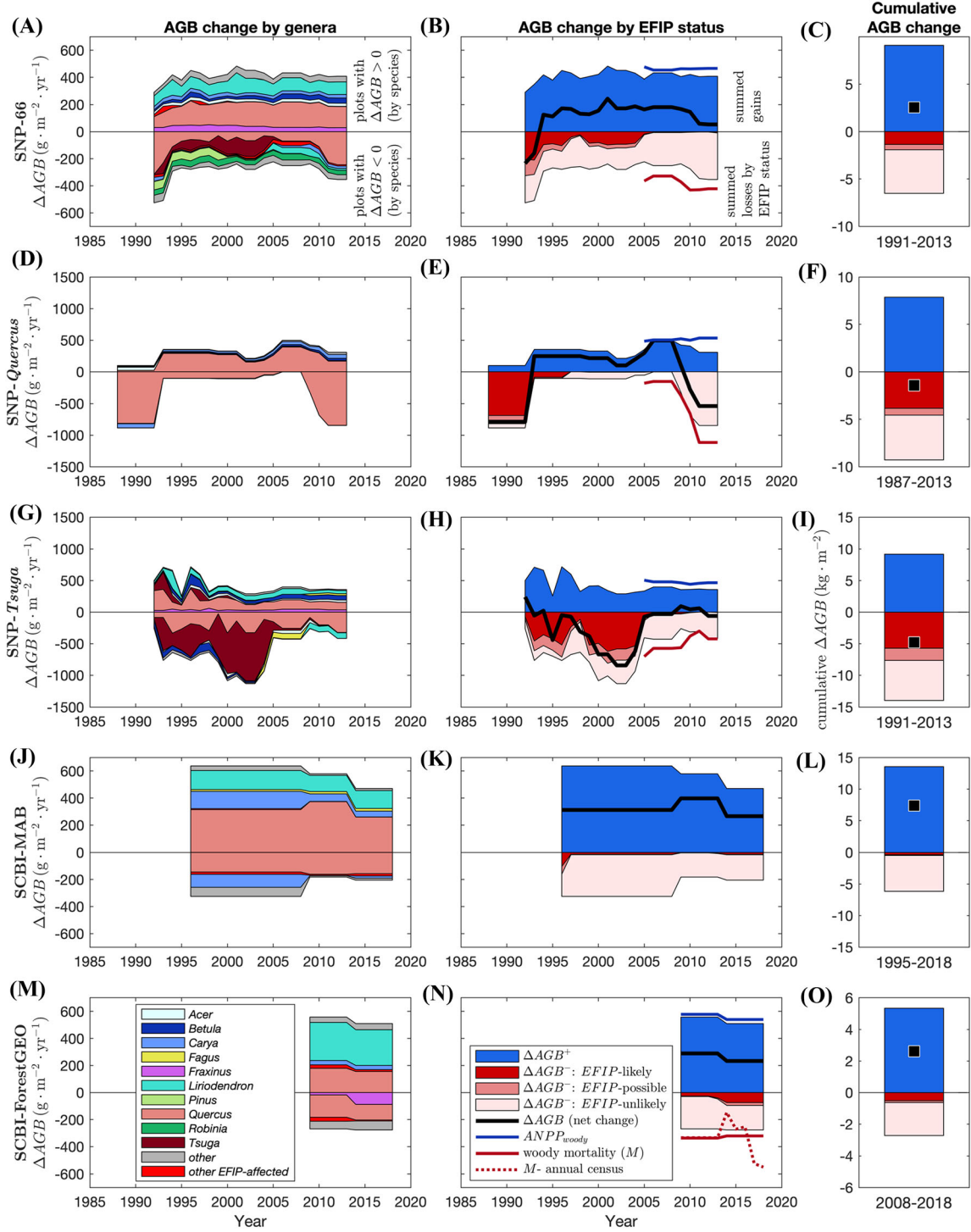


Figure 4. Changes in live aboveground biomass (AGB) by genera and EFIP-status. The first column shows ΔAGB^+ (positive values) and ΔAGB^- (negative values) by genera per plot or quadrat from one census to the next (first column). In the second column, these changes are summed across genera and grouped by the likelihood that the loss was EFIP driven. Total ΔAGB^+ and ΔAGB^- approach but do not equal total woody aboveground net primary productivity ($\text{ANPP}_{\text{woody}}$) and woody mortality (M), respectively (plotted when known). Panel (n) includes woody mortality (DBH ≥ 10 cm only) from the annual mortality census, illustrating the increase in loss rate with the arrival of emerald ash borer. The final column shows cumulative gains and losses across the census period for each plot set. Plot sets are as described in Table 2.

Impacts on Tree Diversity

EFIP-associated declines in individual genera contributed substantively to changes in α - and γ -diversity (Figure 5). Across the SNP-66 plots, α -diversity losses and gains nearly balanced such that the average number of genera per plot declined only 3% from 1991 to 2013 (Figure 5C). EFIP-likely and EFIP-possible losses contributed 23% and 6%, respectively, to α -diversity losses (Figure 5A–C). There was a net change in the total number of genera present in these plots (γ -diversity) of + 2 genera (from 26 to 28). This included a loss of three genera to EFIP (*Castanea*, *Cercis*, and *Tsuga*), stochastic loss of one genus that probably was not affected by EFIP (that is, disappearance of genera known to persist in the region), and stochastic gain of six genera (that is, appearance or reappearance of native tree genera).

Changes in diversity were much more variable within plot sets focused on a single forest type (SNP-*Quercus*, SNP-*Tsuga*, SCBI). In the SNP-*Quercus* plots, which were originally heavily dominated by oaks (83–100% oak biomass), gypsy moth-associated oak mortality led to increased α - and γ -diversity (Figure 5E–H). In contrast, in the SNP-*Tsuga* plots, which had 0.4–55% *Tsuga* biomass, loss of *Tsuga* following hemlock woolly adelgid arrival contributed to declines in both α - and γ -diversity (Figure 5I–L), in part because most regenerating hardwood trees remained below 10 cm DBH. At SCBI, losses of *Cornus*, *Cercis*, *Ulmus*, *Castanea*, and *Fraxinus* contributed to declines in α -diversity, with EFIP-associated losses contributing 47% and 51% to total losses in the SCBI-MAB and SCBI-Forest-GEO plots, respectively (Figure 5N–T). Stochastic losses and gains in α -diversity were approximately balanced at SCBI (Figure 5O, S), and no γ -diversity losses were attributed to EFIP (Figure 5P, T).

DISCUSSION

Over the past century, EFIP have significantly impacted at least eight tree genera—a total of at least 22 species—in the Appalachian/Blue Ridge Mountains ecoregion (Tables 1, S2). This represents 24% of the 33 genera registered in our monitoring plots. Within our long-term monitoring plots, EFIP were associated with notably elevated mortality rates (Figure 2) and steep declines in abundance and AGB (Figure 3; Table 3). With the partial exception of *Quercus* spp., which regained AGB but not abundance following a gypsy moth outbreak (Figure 3A, B), these declines have not been reversed, leaving multiple tree species imperiled (*C.*

dentata, *J. cinerea*, *U. americana*, *T. canadensis*, *Fraxinus* spp.; IUCN 2019). Despite substantial EFIP-associated losses, ecosystem AGB increased and diversity held relatively constant across the full set of SNP plots because less-affected taxa in these relatively diverse temperate forests compensated losses.

Analysis Uncertainty

The precision with which we were able to quantify the impacts of EFIP ranged from extremely coarse for the outbreaks that occurred primarily prior to the initiation of our monitoring plots to high for subsequent outbreaks. Estimates of total losses for the earliest outbreaks (*C. dentata*, *Ulmus* spp., *C. canadensis*, and *J. cinerea*) are necessarily very rough (Tables 3, S3; Appendix S3). Notably, this group includes *C. dentata*, which could contribute up to about 50% of estimated AGB losses over the century scale (Table 3). Although our estimated range of AGB loss aligns with estimates that *C. dentata* historically accounted for about 8–25% of dominant trees in the study region (Karban 1978; Connors 1988; Hanberry and Nowacki 2016), uncertainty remains high. On the other end of the spectrum, *Tsuga* and *Fraxinus* spp. losses to date have been captured with monitoring frequencies of 1–4 years since the beginning of documented EFIP activity (Table 2), and the causal agents have been confirmed by tree-level observations within our plots.

Our approach likely overestimates some aspects of EFIP impacts, while underestimating others. While our analysis should accurately capture the impacts of more virulent and lethal EFIP that kill the majority of adult trees once established in the region (for example, chestnut blight, butternut canker, hemlock woolly adelgid, emerald ash borer) or that contribute to most of the mortality for the host taxa during an outbreak (gypsy moths on *Quercus* spp.), it may mis-attribute some instances of mortality to the EFIP in cases where the EFIP is less virulent and/or lethal (for example, *Neofusicoccum* spp. on *C. canadensis*, Dutch elm disease on *U. rubra*). Additional factors including native pests or pathogens, environmental stress, and natural succession may all contribute to individual mortality and population trends. In particular, it is difficult to know how much *Neofusicoccum* spp. infections have contributed to the decline of *Cercis canadensis*, which remains common in the region despite the long-term presence of the pathogen and may be undergoing successional declines in these aging forest stands.

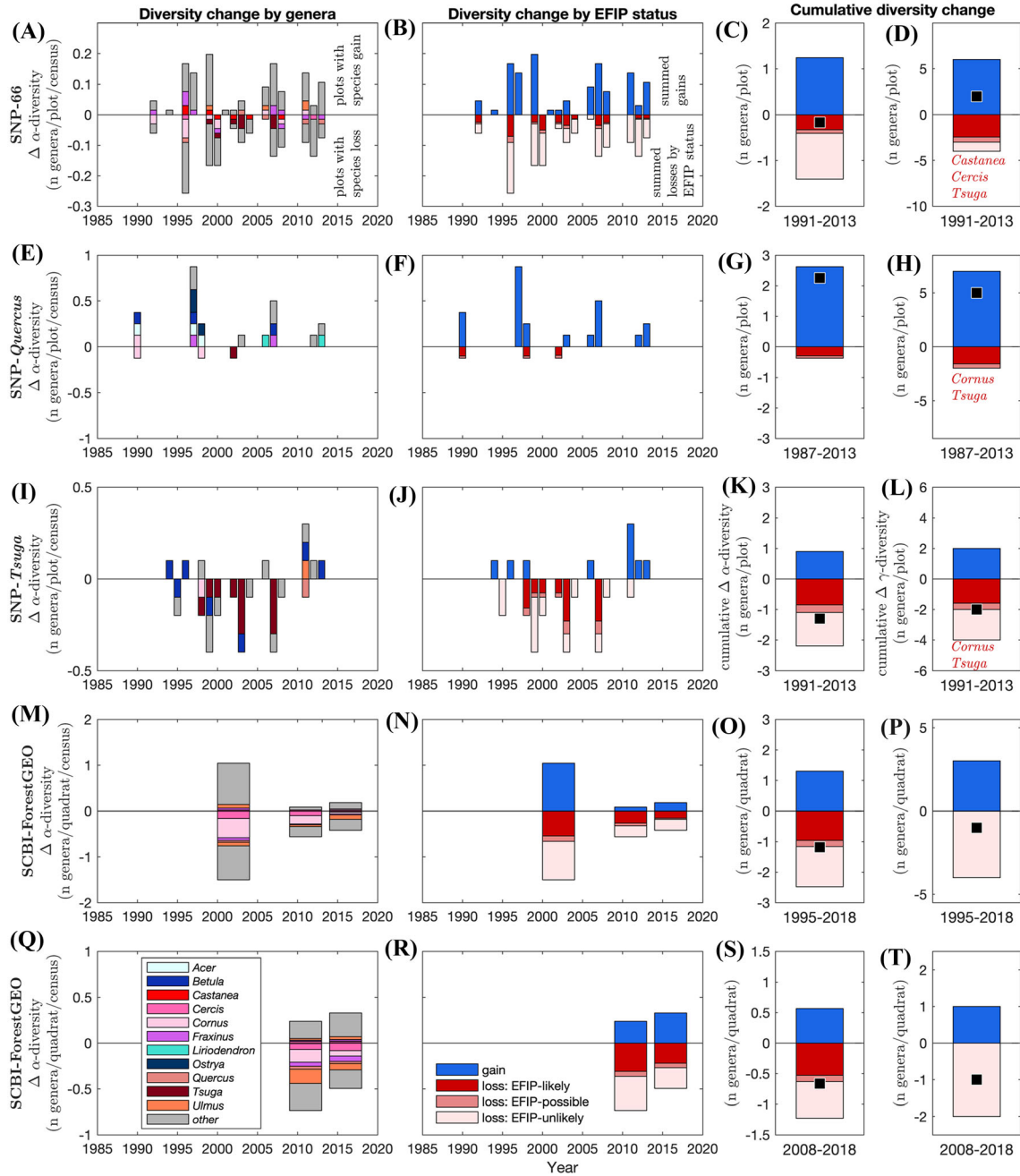


Figure 5. Changes in α - and γ -diversity, including losses driven by invasive insects and pathogens. Shown are changes in the presence or absence of genera (α -diversity) through time, both by genus (first column) and by the likelihood that the loss was EFIP driven (second column). Changes, which are registered at the midpoint of a census interval, are averaged across plots (SNP) or quadrats (ForestGEO); for example, loss of one genus in one SNP-66 plot equates to -0.015 averaged across plots. The third and fourth columns show cumulative change of α -diversity and in the total number of genera across all plots or subplots (γ -diversity), respectively, with γ -diversity plots annotated with the names of EFIP-affected genera that were lost. Plot sets are as described in Table 2.

At the same time that our approach may misattribute some mortality to EFIP, it misses the effects of multiple EFIP known to affect trees within the region (Table S2) and potentially others that could have been missed by our search process.

Documented EFIP that affected trees in the region during our analysis period but were not included in our analysis include balsam woolly adelgid (*Adelges piceae*), which decimated high-elevation populations of *Abies balsamea* within SNP; white pine

blister rust (*Cronartium ribicola*), which has been confirmed on *Pinus strobus*; beech bark disease (*Neonectria* spp.), which has killed *Fagus grandifolia* trees in SNP; thousand cankers disease (*Geosmithia morbida*), which appears to be affecting *Juglans* spp. in our plots; and emerald ash borer on novel host *Chionanthus virginicus* (Cipollini 2015), which has been confirmed in the SCBI-ForestGEO plot. Despite the fact that some of our estimates are necessarily coarse, the broad-scale overview that we derived from available data and historical records provides a unique long-term picture into the magnitude of the impact of EFIP on forest composition, diversity, and AGB.

Impacts on Tree Taxa

All of the EFIP-affected taxa considered here declined in abundance—sometimes precipitously—and have not subsequently recovered. The majority ($n = 5$) of the EFIP considered here have driven their host taxa ($n = 7$) to the IUCN red list of threatened and endangered species (IUCN 2019). *Castanea dentata* (critically endangered) persists mainly as non-reproductive sprouts from old stumps or root systems (Anagnostakis 1987); *Ulmus americana* (endangered) underwent drastic reductions in average lifespan but still persists mainly as smaller individuals. *Juglans cinerea* (endangered) has decreased about 58% across its US range (Morin and others 2018). *Tsuga canadensis* (near-threatened) experience nearly 100% mortality upon exposure to the adelgid, and untreated trees will likely be extirpated from the entire mid-Atlantic region before 2050 (Ellison and others 2018). The three *Fraxinus* species (all critically endangered) undergo nearly 100% mortality of reproductively mature individuals from emerald ash borer (Herms and McCullough 2014; Abella and others 2019). The future survival of these species will likely depend on conservation and restoration actions (for example, Jacobs 2007; Herms and McCullough 2014; Morin and others 2018). In contrast, *U. rubra*, *Quercus* spp., *Cornus* spp., and *Cercis canadensis* remain fairly common and are not currently at risk of extinction (IUCN 2019). Although the continued declines of *U. rubra* and *Cornus* spp. are probably largely attributable to EFIP (Figure 2, Table S4), declines of *Cercis canadensis* may be primarily successional, with some acceleration by the pathogen. Continued declines in *Quercus* spp. abundance are not attributable to gypsy moths, but rather to oak decline and failure to regenerate in closed-canopy forests impacted by

fire suppression, invasive plants, and heavy deer herbivory (Oak and others 2016).

Impacts on Carbon Cycling

Our results indicate that EFIP have been a significant driver of AGB loss to mortality on a multi-decade timescale (Figure 4, Table 3), which complements a recent analysis demonstrating their large regional impact over the past decade (Fei and others 2019). Despite the fact that EFIP were associated with increased biomass mortality in our study plots, average AGB increased (Figures 4, S1). Increasing AGB is typical of forests in the eastern USA, most of which are recovering from past harvesting and/or agricultural activities (McGarvey and others 2014; Zhu and others 2018). Biomass accumulation in the secondary forests analyzed here was at least somewhat curtailed by losses of EFIP-affected taxa, although biomass mortality was often compensated by growth of less-affected taxa (Figure 4). Quantifying the magnitude to which EFIP reduced the net carbon balance of ecosystems in this region, including their impact on forest carbon pools other than AGB (Peltzer and others 2010; Fraterrigo and others 2018), will require representing EFIP impacts in models (Dietze and Matthes 2014). Representation of EFIP-driven mortality in models will be particularly important given that tree mortality is one of the largest uncertainties in projections of future forest dynamics (Bugmann and others 2019) and thereby the future of the terrestrial carbon sink (Friedlingstein and others 2006). Our results demonstrate that representation of EFIP in models is important to accurately characterize forest carbon cycling in this region—particularly considering that EFIP outbreaks are likely to become more prevalent in the future (Levine and D’Antonio 2003; Dukes and others 2009).

Impacts on Tree Diversity

Despite major reductions in abundance for a quarter of the tree genera of the region, tree biodiversity has not changed dramatically in recent decades. In part, this may be explained by the limited temporal scope of our analysis, which misses initial declines in several taxa and captures only the initial stages of decline in *Fraxinus*.

Our analysis shows that EFIP-associated losses on local (α -) diversity can be positive or negative (Figure 5). Mortality can reduce α -diversity if trees that die are not replaced or are replaced by species

already present. This was the case in SNP-*Tsuga* and SCBI plots (Figure 5) and, historically, in an oak–chestnut forest in SNP’s White Oak Canyon following the loss of *Castanea dentata*, which was replaced primarily by *Quercus rubra* (Karban 1978). In some cases, however, mortality of canopy dominants allows more species to establish (Ellison and others 2018)—as observed in SNP-*Quercus* plots (Figure 5). Thus, the lack of any major overall trend in α -diversity across the SNP-66 plots (Figure 5C) is the aggregate of variable local community dynamics.

EFIP have yet to affect the regional species pool. Although three genera (*Castanea*, *Cercis*, *Tsuga*) were lost from the SNP-66 monitoring plots, contributing negatively to observed γ -diversity (Figure 5D), none of these have been extirpated from the region. Such stability in a regional tree species pool has also been observed over four centuries for New England forests (Thompson and others 2013), despite exposure to even more EFIP (Liebhold and others 2013). Thus, despite the often dramatic declines in abundance caused by EFIP, persistence of scattered individuals, often small and non-reproductive, lends stability to the regional species pool.

CONCLUSIONS

Our analysis points to EFIP as a major driver of forest composition, biomass, and diversity over the past century. While our quantitative estimates are specific to our study plots, the Blue Ridge Mountains ecoregion is centrally located within the temperate forest biome of eastern North America and broadly representative in terms of host taxa and EFIP exposure (Liebhold and others 2013; Potter and others 2019). Thus, the observed importance of EFIP to forest dynamics is probably general across the biome (Fei and others 2019). Their impact is likely to be even greater in the future, given the number of nascent EFIP threats combined with continuing introductions and exacerbating effects of climate change (Seidl and others 2018). From a scientific standpoint, ongoing monitoring and model development will be critical to predicting how EFIP will impact future forest dynamics (Dietze and Matthes 2014) and, in turn, Earth’s climate (Friedlingstein and others 2006; Bugmann and others 2019). From the standpoint of forest management and conservation, limiting the spread of invasives on both global and local scales—for example, through strengthened regulations to prevent transport and release of EFIP and enhanced plant biosecurity cyberinfrastructure (Ma-

garey and others 2009)—will yield benefits for biodiversity, climate change mitigation, and other ecosystem services. Meanwhile, the impacts of the inevitable arrival of new EFIP may be moderated through conservation of diverse forests, which may be less susceptible to invasion (Guo and others 2019) and more resistant and resilient to disturbance (Isbell and others 2015); mitigation of climate change, which exacerbates EFIP threats (Ayres and Lombardero 2000; Dukes and others 2009; Seidl and others 2018); control of EFIP, when possible (for example, Hansen and others 2019; McCarty and Addesso 2019); and conservation and restoration of resistant host populations (for example, Jacobs 2007; Herms and McCullough 2014; Morin and others 2018).

ACKNOWLEDGEMENTS

We thank the many researchers who assisted with forest censuses at both SCBI and SNP and local professionals who provided information on pests and pathogens in the region (Rolf Gubler and Dale Meyerhoeffter at SNP; Lori Chamberlin and Katlin Mooneyham at Virginia Department of Forestry). Thank you to Rupert Seidl and anonymous reviewers for helpful comments. This research was funded by Smithsonian’s Forest Global Earth Observatory, the Shenandoah National Park Inventory and Monitoring Program and grants from the Virginia Native Plant Society ($n = 2$) and the Shenandoah National Park Trust.

DATA AVAILABILITY

Data, code, and results associated with this project are archived in Zenodo (Doi: <https://doi.org/10.5281/zenodo.3728134>). <https://doi.org/10.5281/zenodo.3604993> (version of SCBI-ForestGEO data repository used in this analysis, archived on Zenodo). <https://scbi-forestgeo.github.io/SCBI-ForestGEO-Data/> (SCBI-ForestGEO data repository on GitHub). <https://ctfs.si.edu/datarequest/> (SCBI census data through ForestGEO data portal).

REFERENCES

- Abella SR, Hausman CE, Jaeger JF, Menard KS, Schetter TA, Rocha OJ. 2019. Fourteen years of swamp forest change from the onset, during, and after invasion of emerald ash borer. *Biol Invasions* 21:3685–96.
- Anagnostakis SL. 1987. Chestnut blight: The classical problem of an introduced pathogen. *Mycologia* 79:23–37.
- Anderson-Teixeira KJ, Davies SJ, Bennett AC, Gonzalez-Akre EB, Muller-Landau HC, Joseph Wright S, Abu Salim K, Almeyda Zambrano AM, Alonso A, Baltzer JL, Basset Y, Bourg NA, Broadbent EN, Brockelman WY, Bunyavechewin S,

- Burslem DFRP, Butt N, Cao M, Cardenas D, Chuyong GB, Clay K, Cordell S, Dattaraja HS, Deng X, Detto M, Du X, Duque A, Erikson DL, Ewango CEN, Fischer GA, Fletcher C, Foster RB, Giardina CP, Gilbert GS, Gunatilleke N, Gunatilleke S, Hao Z, Hargrove WW, Hart TB, Hau BCH, He F, Hoffman FM, Howe RW, Hubbell SP, Inman-Narahari FM, Jansen PA, Jiang M, Johnson DJ, Kanzaki M, Kassim AR, Kenfack D, Kibet S, Kinnaird MF, Korte L, Kral K, Kumar J, Larson AJ, Li Y, Li X, Liu S, Lum SKY, Lutz JA, Ma K, Maddalena DM, Makana J-R, Malhi Y, Marthews T, Mat Serudin R, McMahon SM, McShea WJ, Memiaghe HR, Mi X, Mizuno T, Morecroft M, Myers JA, Novotny V, de Oliveira AA, Ong PS, Orwig DA, Ostertag R, den Ouden J, Parker GG, Phillips RP, Sack L, Sainge MN, Sang W, Sri-ngernyuan K, Sukumar R, Sun I-F, Sungpalee W, Suresh HS, Tan S, Thomas SC, Thomas DW, Thompson J, Turner BL, Uriarte M, Valencia R, et al. 2015. CTFs-ForestGEO: a worldwide network monitoring forests in an era of global change. *Glob Change Biol* 21:528–49.
- Aukema JE, McCullough DG, Von Holle B, Liebhold AM, Britton K, Frankel SJ. 2010. Historical accumulation of nonindigenous forest pests in the continental United States. *BioScience* 60:886–97.
- Ayres MP, Lombardero MJ. 2000. Assessing the consequences of global change for forest disturbance from herbivores and pathogens. *Sci Total Environ* 262:263–86.
- Berg LY, Moore RB. 1941. Forest cover types of Shenandoah National Park, Virginia. Luray, Virginia, USA: United States Department of the Interior: National Park Service.
- Bonan GB. 2008. Forests and Climate Change: Forcings, Feedbacks, and the Climate Benefits of Forests. *Science* 320:1444–9.
- Bourg NA, McShea WJ, Thompson JR, McGarvey JC, Shen X. 2013. Initial census, woody seedling, seed rain, and stand structure data for the SCBI SIGEO Large Forest Dynamics Plot: *Ecological Archives* E094-195. *Ecology* 94:2111–2.
- Boyd IL, Freer-Smith PH, Gilligan CA, Godfray HCJ. 2013. The consequence of tree pests and diseases for ecosystem services. *Science* 342:1235773.
- Bradshaw CJA, Leroy B, Bellard C, Roiz D, Albert C, Fournier A, Barbet-Massin M, Salles J-M, Simard F, Courchamp F. 2016. Massive yet grossly underestimated global costs of invasive insects. *Nat Commun* 7:12986.
- Brasier CM. 1991. *Ophiostoma novo-ulmi* sp. nov., causative agent of current Dutch elm disease pandemics. *Mycopathologia* 115:151–61.
- Brasier CM. 2000. Intercontinental spread and continuing evolution of the Dutch Elm disease pathogens. In: Dunn CP, Ed. *The Elms: breeding, conservation, and disease management*. Boston, MA: Springer. pp 61–72. https://doi.org/10.1007/978-1-4615-4507-1_4
- Bugmann H, Seidl R, Hartig F, Bohn F, Bruna J, Cailleret M, François L, Heinke J, Henrot A-J, Hickler T, Hülsmann L, Huth A, Jacquemin I, Kollas C, Lasch-Born P, Lexer MJ, Merganič J, Merganičová K, Mette T, Miranda BR, Nadal-Sala D, Rammer W, Rammig A, Reineking B, Roedig E, Sabaté S, Steinkamp J, Suckow F, Vacchiano G, Wild J, Xu C, Reyer CPO. 2019. Tree mortality submodels drive simulated long-term forest dynamics: assessing 15 models from the stand to global scale. *Ecosphere* 10:e02616.
- Caetano-Anollés G, Trigliano RN, Windham MT. 2001. Patterns of evolution in *Discula* fungi and the origin of dogwood anthracnose in North America, studied using arbitrarily amplified and ribosomal DNA. *Curr Genet* 39:346–54.
- Carr DE, Banas LE. 2000. Dogwood anthracnose (*Discula destructiva*): effects of and consequences for Host (*Cornus florida*) demography. *Am Midl Nat* 143:169–77.
- Cass W, Hochstedler W, Fisichelli N. 2011. Shenandoah National Park forest vegetation monitoring protocol: Version 2.3. Natural Resource Report NPS/MIDN/NRR—2011/475. :52.
- Cass W, Hochstedler WW, Williams AB. 2012. Forest vegetation status in Shenandoah National Park: long-term ecological monitoring summary report 2003–2011. Natural resources data series NPS/MIDN/NRDS-2012/353. Fort Collins, CO: National Park Service.
- Chojnacky DC, Heath LS, Jenkins JC. 2014. Updated generalized biomass equations for North American tree species. *Forestry* 87:129–51.
- Cipollini D. 2015. White fringetree as a novel larval host for Emerald Ash Borer. *J Econ Entomol* 108:370–5.
- Connors JA. 1988. Shenandoah National Park: an interpretive guide. Blacksburg, VA: McDonald & Woodward Pub Co.
- Dietze MC, Matthes JH. 2014. A general ecophysiological framework for modelling the impact of pests and pathogens on forest ecosystems. *Ecol Lett* 17:1418–26.
- Dukes JS, Pontius J, Orwig D, Garnas JR, Rodgers VL, Brazee N, Cooke B, Theoharides KA, Stange EE, Harrington R, Ehrenfeld J, Gurevitch J, Lerdau M, Stinson K, Wick R, Ayres M. 2009. Responses of insect pests, pathogens, and invasive plant species to climate change in the forests of northeastern North America: what can we predict? *Can J For Res* 39:231–48.
- Ellison AM, Orwig DA, Fitzpatrick MC, Preisser EL. 2018. The past, present, and future of the hemlock woolly adelgid (*Adelges tsugae*) and its ecological interactions with eastern hemlock (*Tsuga canadensis*) forests. *Insects* 9:172.
- Fei S, Morin RS, Oswalt CM, Liebhold AM. 2019. Biomass losses resulting from insect and disease invasions in US forests. *Proc Natl Acad Sci* 116:17371–17376.
- Finzi AC, Raymer PCL, Giasson M-A, Orwig DA. 2014. Net primary production and soil respiration in New England hemlock forests affected by the hemlock woolly adelgid. *Ecosphere* 5:art98.
- Flower CE, Knight KS, Gonzalez-Meler MA. 2013. Impacts of the emerald ash borer (*Agrilus planipennis* Fairmaire) induced ash (*Fraxinus* spp.) mortality on forest carbon cycling and successional dynamics in the eastern United States. *Biol Invasions* 15:931–44.
- Fraterrigo JM, Ream K, Knoepp JD. 2018. Tree mortality from insect infestation enhances carbon stabilization in Southern Appalachian forest soils. *J Geophys Res Biogeosci* 123:2121–34.
- Friedlingstein P, Cox P, Betts R, Bopp L, von Bloh W, Brovkin V, Cadule P, Doney S, Eby M, Fung I, Bala G, John J, Jones C, Joos F, Kato T, Kawamiya M, Knorr W, Lindsay K, Matthews HD, Raddatz T, Rayner P, Reick C, Roeckner E, Schnitzler K-G, Schnur R, Strassmann K, Weaver AJ, Yoshikawa C, Zeng N. 2006. Climate-carbon cycle feedback analysis: results from the C4MIP model intercomparison. *J Clim* 19:3337–53.
- Gonzalez-Akre E, Meakem V, Eng C-Y, Tepley AJ, Bourg NA, McShea W, Davies SJ, Anderson-Teixeira K. 2016. Patterns of tree mortality in a temperate deciduous forest derived from a large forest dynamics plot. *Ecosphere* 7:e01595.
- Guo Q, Fei S, Potter KM, Liebhold AM, Wen J. 2019. Tree diversity regulates forest pest invasion. *Proc Natl Acad Sci* 116:7382–7386.

- Hanberry BB, Nowacki GJ. 2016. Oaks were the historical foundation genus of the east-central United States. *Quat Sci Rev* 145:94–103.
- Hansen E, Reeser P, Sutton W, Kanaskie A, Navarro S, Goheen EM. 2019. Efficacy of local eradication treatments against the sudden oak death epidemic in Oregon tanoak forests. Woodward S, editor. *For Pathol* 49:e12530.
- Hassan RM, Scholes RJ, Ash N. Millennium Ecosystem Assessment (Program). Eds. 2005. Ecosystems and human well-being: current state and trends: findings of the condition and trends Working Group of the Millennium Ecosystem Assessment. Washington, DC: Island Press.
- Herms DA, McCullough DG. 2014. Emerald Ash Borer invasion of North America: history, biology, ecology, impacts, and management. *Annu Rev Entomol* 59:13–30.
- Isbell F, Craven D, Connolly J, Loreau M, Schmid B, Beierkuhnlein C, Bezemer TM, Bonin C, Bruehlheide H, Luca E de, Ebeling A, Griffin JN, Guo Q, Hautier Y, Hector A, Jentsch A, Kreyling J, Lanta V, Manning P, Meyer ST, Mori AS, Naeem S, Niklaus PA, Polley HW, Reich PB, Roscher C, Seabloom EW, Smith MD, Thakur MP, Tilman D, Tracy BF, Putten WH van der, Ruijven J van, Weigelt A, Weisser WW, Wilsey B, Eisenhauer N. 2015. Biodiversity increases the resistance of ecosystem productivity to climate extremes. *Nature* 526:574–7.
- IUCN. 2019. The IUCN Red List of threatened species. Version 2019-2. <https://www.iucnredlist.org>. Downloaded on 18 August 2019.
- Jacobs DF. 2007. Toward development of silvical strategies for forest restoration of American chestnut (*Castanea dentata*) using blight-resistant hybrids. *Biol Conserv* 137:497–506.
- Jenkins JC, Chojnacky DC, Heath LS, Birdsey RA. 2003. National-scale biomass estimators for United States tree species. *For Sci* 49:12–35.
- Karban R. 1978. Changes in an oak-chestnut forest since the chestnut blight. *Castanea* 43:221–8.
- Kasbohm JW. 1994. Response of black bears to gypsy moth infestation in Shenandoah National Park, Virginia. <https://vt.echworks.lib.vt.edu/handle/10919/39530>. Accessed 05 June 2018.
- Levine JM, D'Antonio CM. 2003. Forecasting biological invasions with increasing international trade. *Conserv Biol* 17:322–6.
- Liebold AM, McCullough DG, Blackburn LM, Frankel SJ, Holle BV, Aukema JE. 2013. A highly aggregated geographical distribution of forest pest invasions in the USA. *Divers Distrib* 19:1208–16.
- Lovett GM, Canham CD, Arthur MA, Weathers KC, Fitzhugh RD. 2006. Forest ecosystem responses to exotic pests and pathogens in eastern North America. *BioScience* 56:395.
- Lovett GM, Weiss M, Liebold AM, Holmes TP, Leung B, Lambert KF, Orwig DA, Campbell FT, Rosenthal J, McCullough DG, Wildova R, Ayres MP, Canham CD, Foster DR, LaDeau SL, Weldy T. 2016. Nonnative forest insects and pathogens in the United States: impacts and policy options. *Ecol Appl* 26:1437–55.
- Magarey RD, Colunga-Garcia M, Fieselmann DA. 2009. Plant biosecurity in the United states: roles, responsibilities, and information needs. *BioScience* 59:875–84.
- Mahan CG, Diefenbach DR, Cass WB. 2007. Evaluating and revising a long-term monitoring program for vascular plants: lessons from Shenandoah National Park. *Nat Areas J* 27:16–24.
- McCarty EP, Adesso KM. 2019. Hemlock woolly adelgid (Hemiptera: Adelgidae) management in forest, landscape, and nursery production. *J Insect Sci* 19. 19:iez031. <https://doi.org/10.1093/jisesa/iez031>.
- McGarvey JC, Thompson JR, Epstein HE, Shugart HH. 2014. Carbon storage in old-growth forests of the Mid-Atlantic: toward better understanding the eastern forest carbon sink. *Ecology* 96:311–7.
- Morin RS, Gottschalk KW, Ostry ME, Liebhold AM. 2018. Regional patterns of declining butternut (*Juglans cinerea* L.) suggest site characteristics for restoration. *Ecol Evol* 8:546–59.
- Oak SW, Spetich MA, Morin RS. 2016. Oak decline in central hardwood forests: frequency, spatial extent, and scale. In: Greenberg CH, Collins BS, Eds. Natural disturbances and historic range of variation. managing forest ecosystems. Cham: Springer. pp 49–71. https://doi.org/10.1007/978-3-319-21527-3_3. Accessed 21 Jan 2016.
- Peltzer DA, Allen RB, Lovett GM, Whitehead D, Wardle DA. 2010. Effects of biological invasions on forest carbon sequestration. *Glob Change Biol* 16:732–46.
- Potter K, Escanferla M, Jetton R, Man G. 2019. Important insect and disease threats to United States tree species and geographic patterns of their potential impacts. *Forests* 10:304.
- Sakalidis ML, Slippers B, Wingfield BD, Hardy GESJ, Burgess TI. 2013. The challenge of understanding the origin, pathways and extent of fungal invasions: global populations of the *Neofusicoccum parvum*–*N. ribis* species complex. *Divers Distrib* 19:873–83.
- Sala OE. 2000. Global biodiversity scenarios for the year 2100. *Science* 287:1770–4.
- Seidl R, Klonner G, Rammer W, Essl F, Moreno A, Neumann M, Dullinger S. 2018. Invasive alien pests threaten the carbon stored in Europe's forests. *Nat Commun* 9:1626.
- Strayer DL, Eviner VT, Jeschke JM, Pace ML. 2006. Understanding the long-term effects of species invasions. *Trends Ecol Evol* 21:645–51.
- Thompson JR, Carpenter DN, Cogbill CV, Foster DR. 2013. Four centuries of change in northeastern United States forests. *PLOS ONE* 8:e72540.
- Wester HV, Davidson RW, Fowler ME. 1950. Cankers of Linden and Redbud. *Plant Dis Rep*. 34. <https://www.cabdirect.org/cabdirect/abstract/19511100348>. Accessed 19 Mar 2019.
- Young JG, Fleming W, Cass WB, Lea C. 2009. Vegetation of Shenandoah National Park in relation to environmental gradients, version 2.0. Philadelphia, PA: National Park Service. <https://irma.nps.gov/DataStore/DownloadFile/440196>. Accessed 30 Mar 2019.
- Zhu K, Zhang J, Niu S, Chu C, Luo Y. 2018. Limits to growth of forest biomass carbon sink under climate change. *Nat Commun* 9:2709.